

## Supporting Information

# Polyaniline Nanofiber/Electrochemically Reduced Graphene Oxide Layer-by-Layer Electrodes for Electrochemical Energy Storage

*Ju-Won Jeon, Se Ra Kwon and Jodie L. Lutkenhaus\**

Artie McFerrin Department of Chemical Engineering, Texas A&M University, 3122 TAMU,  
College Station, TX, 77843-3122, United States

To which all correspondences should be addressed: [jodie.lutkenhaus@che.tamu.edu](mailto:jodie.lutkenhaus@che.tamu.edu)

---

Figure S1. Zeta potential of GO dispersion	S6
Figure S2. Digital images of (PANI NF <sub>2.5</sub> /GO <sub>3.5</sub> ) LbL films	S6
Figure S3. Adsorbed mass by QCM	S7
Figure S4. SEM image of drop-cast GO sheets	S7
Figure S5. XPS spectra of PANI NFs and GO sheets	S8
Figure S6. Preconditioning of (PANI NF <sub>2.5</sub> /ERGO <sub>3.5</sub> ) LbL electrode	S8
Figure S7. Forwards and backwards cyclic voltammograms of (PANI NF <sub>2.5</sub> /ERGO <sub>3.5</sub> )	S9
Figure S8. Cyclic voltammograms of (PANI NF <sub>2.5</sub> /ERGO <sub>3.5</sub> ) LbL electrodes at 30 mV/s	S9
Figure S9. Graphs of log i vs. log v	S10
Figure S10. Graphs of $i/v^{0.5}$ vs. $v^{0.5}$	S11
Figure S11. The diffusion-controlled contribution separated from CVs at 5 mV/s	S12
Figure S12. Graphs of $1/q$ vs. $v^{0.5}$ and $q$ vs. $v^{-0.5}$	S13
Figure S13. Cycling stability of 483 nm thick PANI NF electrode at 22 A/g	S14
Table S1. Capacities of (PANI NF <sub>2.5</sub> /ERGO <sub>3.5</sub> ), PAN NF and ERGO	S14

## **Experimental section**

### **Materials**

Aniline, ammonium peroxydisulfate, propylene carbonate, lithium perchlorate, potassium permanganate, (3-aminopropyl)triethoxysilane (APTES), and sodium nitrate were purchased from Sigma Aldrich. Graphite (SP-1) was purchased from Bay Carbon. Lithium foil and Indium-tin oxide (ITO)-coated glass (resistance < 20 ohms) were purchased from Alfa Aesar and Delta Technologies, respectively. Separator (Celgard 3501) was provided by Celgard.

### **Synthesis of polyaniline nanofibers (PANI NFs)**

PANI NFs were synthesized using a previously reported method.<sup>1</sup> Aniline (1.49 g) was dissolved in 1M HCl of 50 ml. Ammonium peroxydisulfate (0.915 g) was dissolved in 1M HCl of 50 ml, separately. Before synthesis, each solution was purged with nitrogen for more than 30 min. Then, the ammonium peroxydisulfate solution was rapidly mixed with the aniline solution under nitrogen at room temperature. The reaction was performed for 24 h. After polymerization, dialysis against deionized water was employed to remove remaining initiator (ammonium peroxydisulfate) and unreacted monomer (aniline) for at least 24 h. The yield of PANI NFs with respect to aniline monomer was approximately 17 wt%. The concentration was adjusted to 0.5 g/ml by adding deionized water for LbL assembly. The PANI NF dispersion was stable in acidic aqueous solution (pH 2.5) for a week. Therefore, synthesized PANI NFs were used within a few days following dilution.

### **Synthesis of graphene oxide (GO) sheets**

First, graphite oxide was synthesized using modified Hummer's method.<sup>2</sup> Graphite power (SP-1, 3 g) and NaNO<sub>3</sub> (2.5 g) were added into concentrated H<sub>2</sub>SO<sub>4</sub> (120 ml), and stirred for 5 h in an

ice water bath.  $\text{KMnO}_4$  (15 g) was slowly added to the above mixture for 30 min while stirring. During  $\text{KMnO}_4$  addition, the temperature of the mixture was maintained below 20 °C using ice. Then, the above mixture was stirred at 35 °C for 2h, and slowly diluted with 250 ml chilled deionized water. Deionized water (700 ml) was added to the above dispersion in an ice water bath. Then, 30 wt%  $\text{H}_2\text{O}_2$  (20 ml) was added to the above mixture. In this process, the color of the dispersion changed from black to brown. For washing, the dispersion was mixed with 5 wt% HCl (1 L), and stirred for several hours. It was dried and dialyzed against deionized water for at least three days to remove the residual salt. Graphite oxide powder was obtained after drying at 60 °C under vacuum condition. The synthesized graphite powder was dissolved in deionized water and sonicated at 100 W for 30 min to yield GO sheets. Chemically reduced GO (CRGO) was prepared by reduction of GO dispersion using hydrazine in basic aqueous solution. After reduction, dialysis was performed in pH 10 water.

### **Layer-by-layer assembly**

The synthesized PANI NFs and GO sheets were diluted to a concentration of 0.5 mg/ml in deionized water. The pH of the PANI NF dispersion was adjusted to 2.5 using HCl; to prevent aggregation, sonication was carried out for 30 min. The GO dispersion was also diluted to 0.5 mg/ml in deionized water, and HCl and NaOH were used to adjust the pH.

PANI NF/GO LbL films were assembled on APTES-treated ITO-coated glass substrates. For APTES treatment, ITO-coated glass substrates were cleaned by sequential sonication in dichloromethane, acetone, methanol, and deionized water for 15 min each. After washing, ITO-coated glass was dried using high-velocity nitrogen gas and dried in a convection oven. Plasma treatment (Harrick PDC-32G) was carried out on dry ITO-coated glass slides for 5 min; then, they were immediately immersed in 2 vol % APTES in toluene for 30 min at 75 °C.<sup>3</sup> After

APTES treatment, the ITO-coated glass was washed with toluene, ethanol, and deionized water, separately. The APTES-treated slides were dried using high velocity nitrogen followed by heating for 15 min at 110 °C.

For LbL assembly, APTES-treated ITO-coated glass substrates were immersed in graphene oxide dispersion for 15 min, and rinsed with deionized water for 2, 1, and 1 min each. The pH of the rinse baths following GO exposure was matched to that of the pH of the GO dispersion. Then, the substrates were immersed in pH 2.5 PANI NF dispersion for 15 min, and rinsed with pH 2.5 deionized water for 2, 1, and 1 min each. The same procedure was repeated until the desired thickness was achieved. For deposition onto cotton fabric, the fabric was immersed in pH 2 water before LbL assembly. In this case, a wringing step was included between the last washing step and the next immersion in dispersion. Other procedures were kept identical.

### **Characterization**

The thickness of PANI NF/GO LbL films was measured using profilometry (P-6, KLA-Tencor), and at least five different locations were measured and averaged. Quartz crystal microbalance (QCM) was employed to measure the mass of the LbL films. A 5 MHz Ti/Au quartz crystal was plasma-treated for 5 min. Then, the PANI NF/GO LbL film was assembled onto the quartz crystal using the assembly process described previously. To determine the composition of PANI NF/GO LbL films, the change in frequency was monitored during each layer deposition from 10 to 15 layer pairs. The frequency was converted to mass using the Sauerbrey equation. The incremental mass of PANI NF and GO layers was 8.4 and 2  $\mu\text{g}/\text{cm}^2$ , respectively. From these incremental masses, the weight fraction of PANI NFs and GO sheets was estimated. Zeta-potential was measured using a Zetasizer (Nano ZS90, Malvern Instruments). UV-vis spectroscopy was performed using a Hitachi U-4100 spectrometer. X-ray photoelectron

spectroscopy (XPS), (Kratos Axis Ultra DLD) was employed with a monochromatic Al (10 mA, 12 kV) X-ray source. To remove charging effects, the C 1s peak (284.5 eV) was used as a reference. Raman spectra (excited at 633 nm) were recorded using Horiba Jobin-Yvon LabRam Raman Confocal Microscope. The baseline correction was performed using Origin.

### **Electrochemical tests**

After LbL assembly, LbL films were dried in a hood for 24 h, and the vacuum-dried for 10 min. The electrochemical tests were carried out using either a three-electrode cell or a two-electrode sandwich-type cell. For the three-electrode cell, the LbL-coated ITO slide was used as the working electrode, and lithium ribbons were used as counter and reference electrodes; 0.5 M LiClO<sub>4</sub> dissolved in propylene carbonate was used as an electrolyte. For the sandwich-type cell, LbL film on ITO-coated glass and lithium ribbon were used as working electrode and counter/reference electrodes, respectively. A separator was sandwiched between the LbL cathode and lithium anode, and 1 M LiClO<sub>4</sub> dissolved in propylene carbonate was used as an electrolyte.<sup>3</sup> All electrochemical tests were performed at room temperature in an oxygen-free and water-free argon-filled glove box. Electrochemical performance such as capacity, specific energy, and specific power were calculated based on the mass of the LbL film alone. Before measurements, electrochemical reduction at 1.5 V and conditioning (one hundred scans from 1.5 to 4.2 V at 20 mV/s) were conducted. The active area for the two-electrode cell and the three-electrode cell was 2 cm<sup>2</sup>. Typical electrode thicknesses for the three-electrode and two-electrode cells ranged from 347 to 1520 nm.

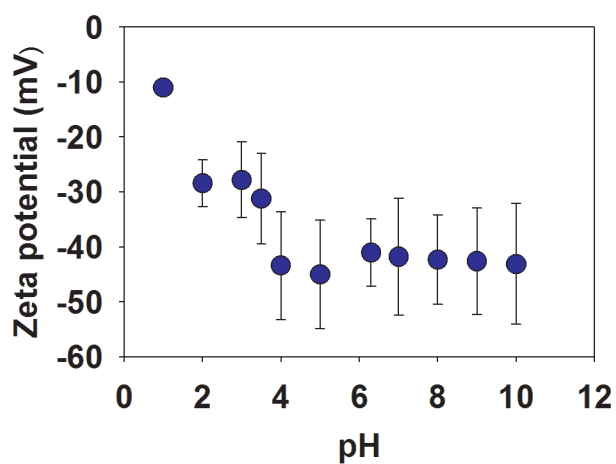


**Figure S1.** Zeta potential of GO sheets dispersed in water at different pH values.

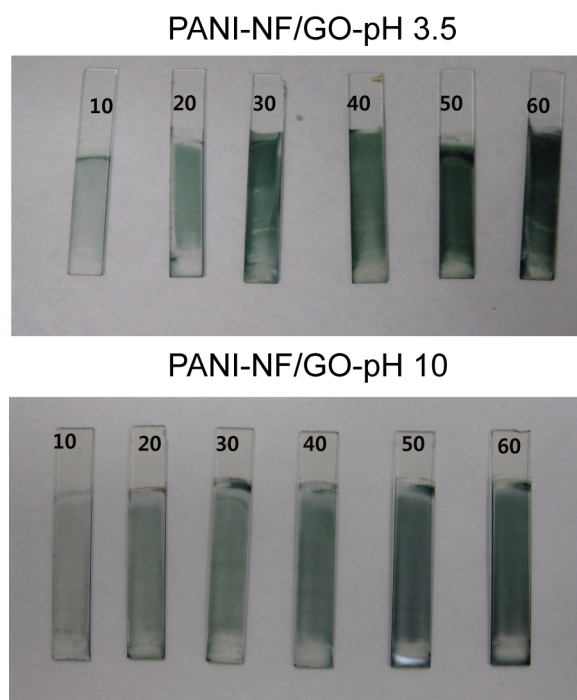


**Figure S2.** Digital images of PANI NF/GO LbL films on ITO-coated glass. The labels denote the number of layer pairs deposited.

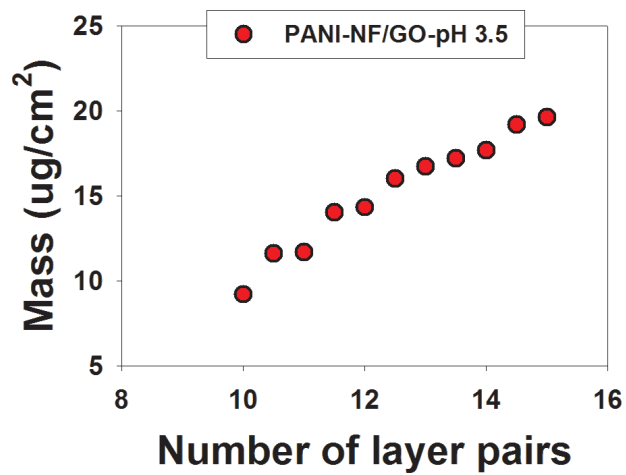


**Figure S3.** Adsorbed mass of (PANI-NF<sub>2.5</sub>/ERGO<sub>3.5</sub>) LbL electrodes measured using quartz crystal microbalance.

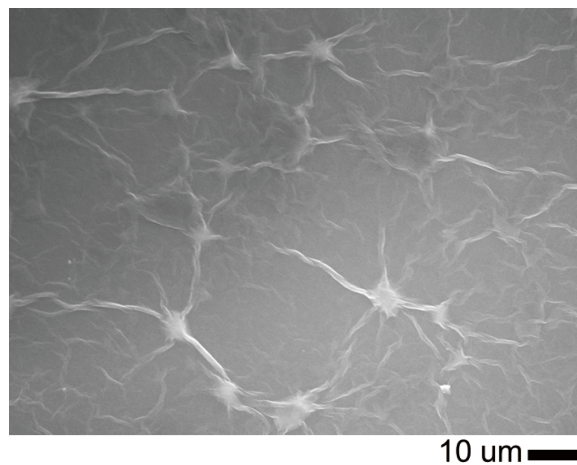


**Figure S4.** Scanning electron micrograph of drop-cast GO sheets.

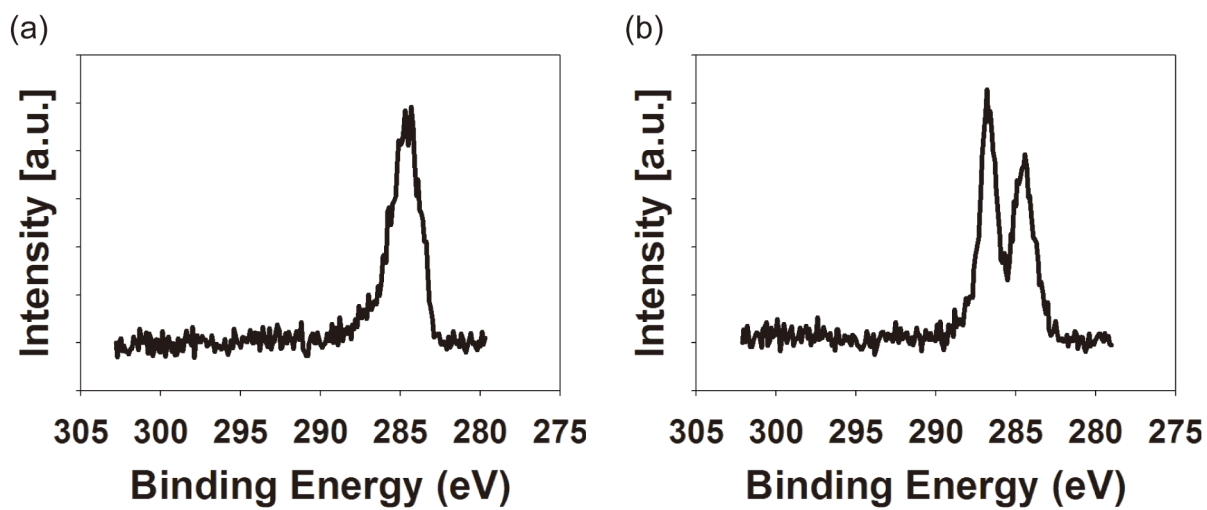


**Figure S5.** XPS of (a) PANI NFs and (b) GO sheets.

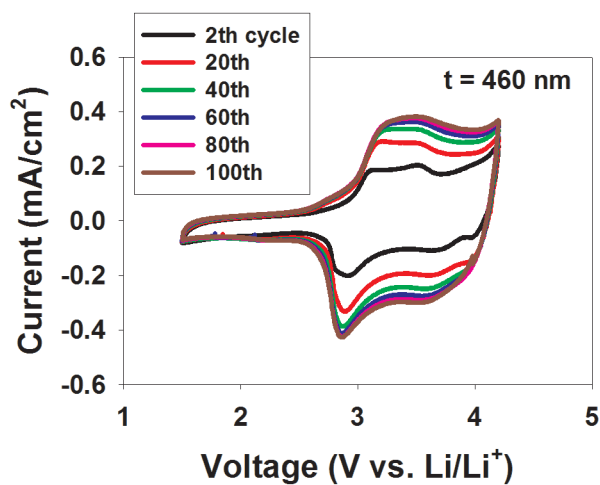


**Figure S6.** Conditioning of a 460 nm thick (PANI-NF<sub>2.5</sub>/ERGO<sub>3.5</sub>) LbL electrode at 20 mV/s.



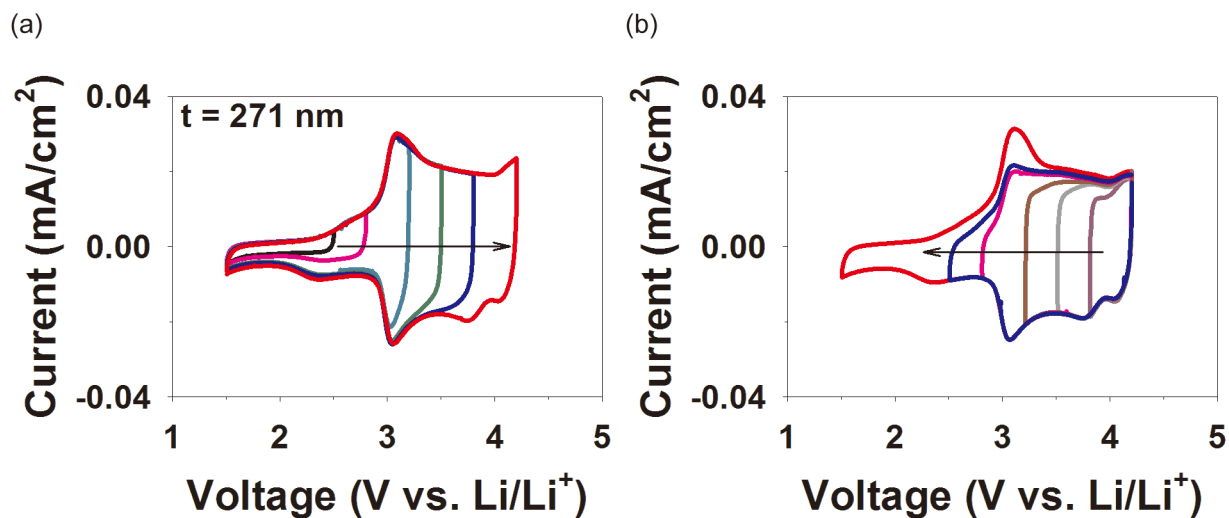


**Figure S7.** (a) Forward and (b) backward scans of cyclic voltammograms for a 271 nm thick (PANI-NF<sub>2.5</sub>/ERGO<sub>3.5</sub>) LbL electrode at 1 mV/s.

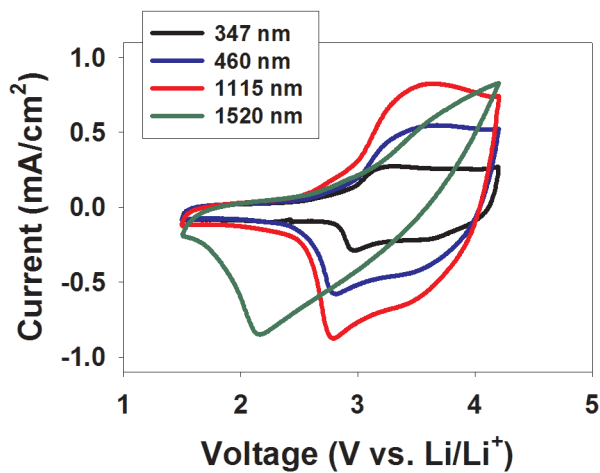


**Figure S8.** Cyclic voltammograms of (PANI-NF<sub>2.5</sub>/ERGO<sub>3.5</sub>) LbL electrodes having various thicknesses at a scan rate of 30 mV/s.

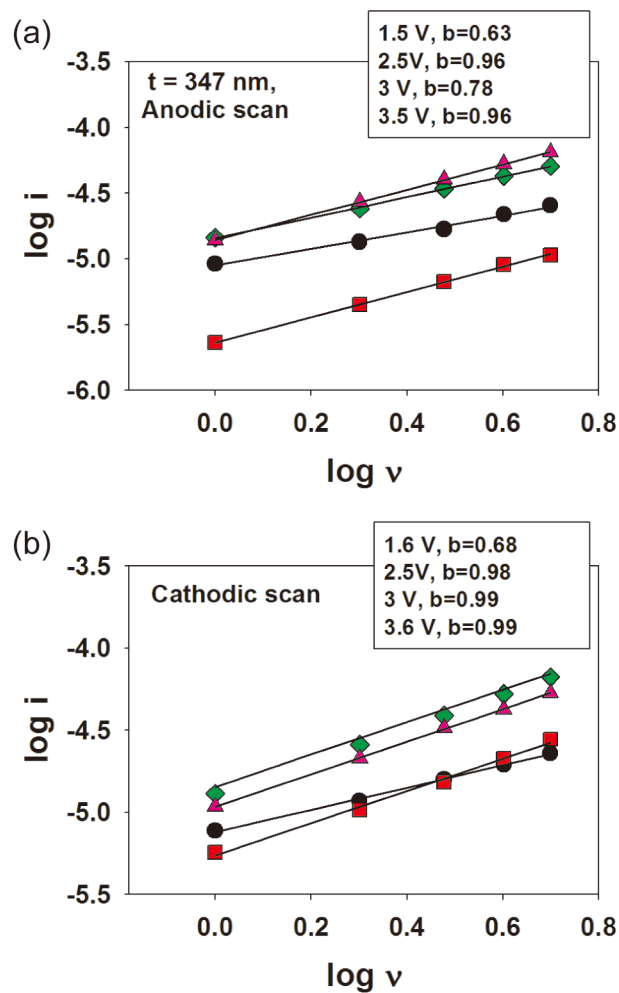


**Figure S9.** Graphs of  $\log i$  vs.  $\log v$  for (a) anodic and (b) cathodic scans of the 347 nm thick (PANI-NF<sub>2.5</sub>/ERGO<sub>3.5</sub>) LbL electrodes used to obtain b values. The calculation was performed using cyclic voltammograms from 1 to 5 mV/s.

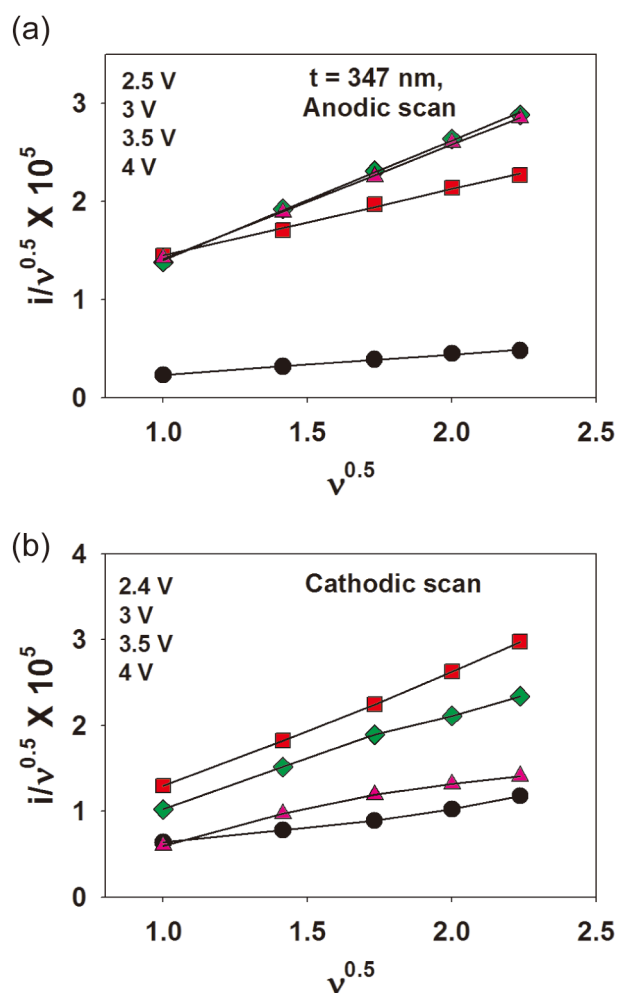


**Figure S10.** Graphs of  $\log i/v^{0.5}$  vs.  $v^{0.5}$  for (a) anodic and (b) cathodic scans of the 347 nm thick (PANI-NF<sub>2.5</sub>/ERGO<sub>3.5</sub>) LbL electrode to separate the diffusion-controlled redox processes. The calculation was performed using cyclic voltammograms from 1 to 5 mV/s.

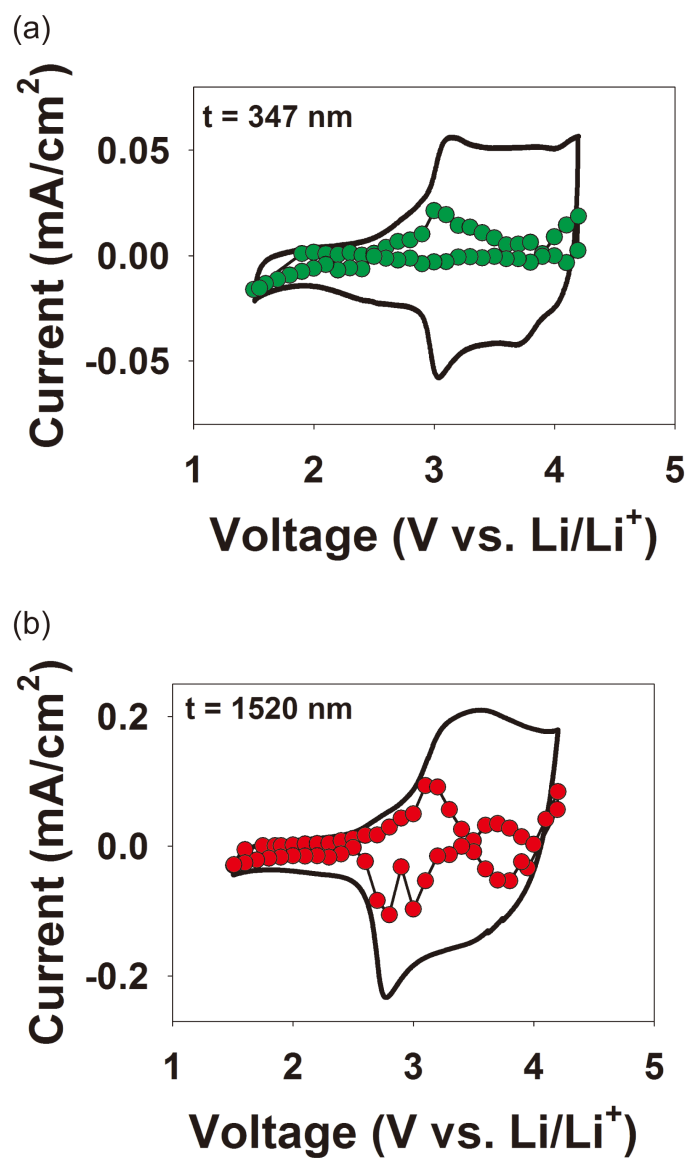


**Figure S11.** The diffusion-controlled contribution separated from cyclic voltammograms of (a) 347 nm and (b) 1520 nm thick (PANI NF<sub>2.5</sub>/ERGO<sub>3.5</sub>) LbL electrodes at 5 mV/s. The dotted line indicates the diffusion-controlled redox processes, and the solid line indicates the total current.

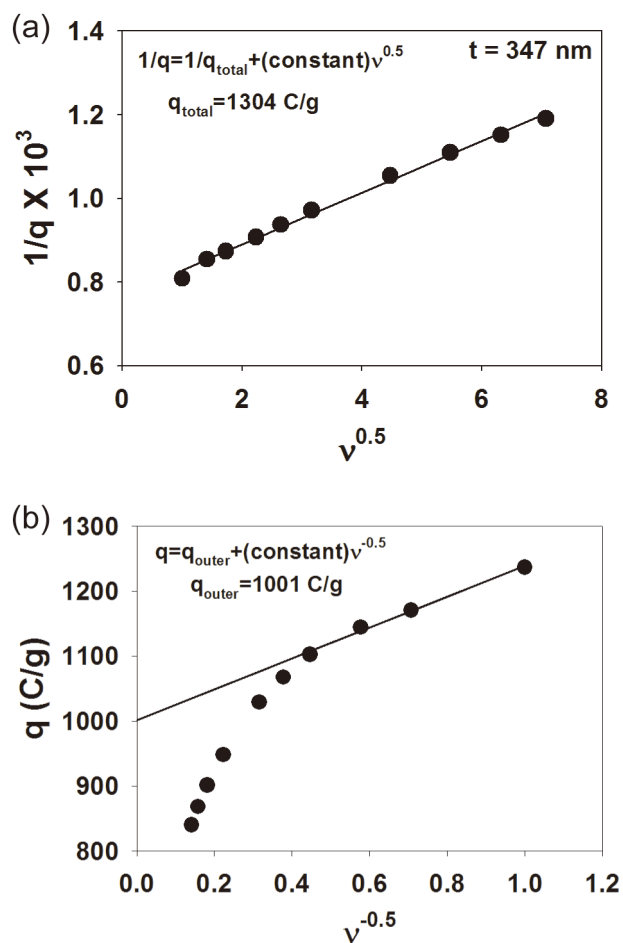


**Figure S12.** Graphs of (a)  $1/q$  vs.  $v^{0.5}$  for  $q_{\text{total}}$ , and (b)  $q$  vs.  $v^{-0.5}$  for  $q_{\text{outer}}$ . The fit presented in panel (b) was executed for low scan rates, as suggested by Sathiya, *J. Am. Chem. Soc.* 2011, 16291.

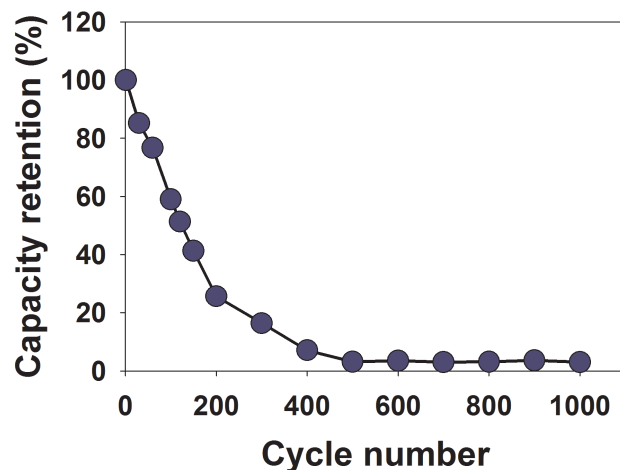


**Figure S13.** Cycling stability of a 483 nm thick PANI NF electrode at 22 A/g.

**Table S1.** Capacity of PANI NF/ERGO, PANI NF, and ERGO at a different current (mAh/g)

	0.03 A/g	0.05 A/g	0.1 A/g	0.5 A/g	1 A/g	2 A/g	3 A/g	5 A/g	7 A/g	10 A/g
PANF/ERGO- 1371 nm				328	309	297	289	275	264	250
PANF/ERGO- 460 nm			461	432	421	408	400	387	378	368
PANF/ERGO- 910 nm	206	195	188	177	171	162	154	141	129	115
PANF/ERGO- 1520 nm	220	215	210	195	183	166	151	125	101	62
PANI NF-483 nm				195	185	176	168	162	158	153
ERGO- 86 nm			186	106	84	65	56	46	41	37

#### Reference

1. J. X. Huang and R. B. Kaner, *Angew. Chem.-Int. Edit.*, 2004, **43**, 5817-5821.
2. W. S. Hummers and R. E. Offeman, *J. Am. Chem. Soc.*, 1958, **80**, 1339-1339.
3. J. W. Jeon, J. O'Neal, L. Shao and J. L. Lutkenhaus, *ACS Appl. Mater. Interfaces*, 2013, **5**, 10127-10136.